ISSN: 2664-9640

Research on MPC-based Wheel Slip Turning Trajectory Tracking Control

Shengguo Zhai, Xuejian Jiao, Huailu Jiang and Dong Zou

School of Shandong University of Technology, Shandong 255000, China.

Abstract

This article addresses the lateral control problem for trajectory tracking of a four-wheel slippage steering small unmanned vehicle, and proposes a control strategy based on model predictive control (MPC). First, a dynamic model of the small unmanned vehicle is established, and a trajectory tracking controller using the model predictive control algorithm is designed based on this model. To verify the effectiveness of the designed controller, a joint simulation experiment using MATLAB and CarSim is conducted. The simulation results show that the designed trajectory tracking controller can be effectively used for trajectory tracking of a wheeled small unmanned vehicle.

Keywords

Wheel slip turning; dynamic model; model predictive control; trajectory tracking.

1. Introduction

With the development of autonomous driving technology, more and more small unmanned vehicles are entering our daily lives. One of them is the skid-steering vehicle, which has a relatively simple structure and can achieve turning in place without a dedicated steering mechanism, making it widely used in outdoor environments. The key aspect of autonomous driving is tracking control, and the control algorithm should maximize the tracking accuracy and driving stability of the unmanned vehicle while ensuring safety[1]. Skid-steering vehicles achieve steering by controlling the differential wheel speed or differential torque applied to the wheels on both sides of the same axle. Due to wheel slipping, the motion of skid-steering vehicles has more uncertainties compared to vehicles with dedicated steering mechanisms[2]. The precise control of autonomous vehicles becomes complex due to the non-linear vehicle model. The main goals of control technology are to improve adaptability, robustness, and accuracy, making the application of control algorithms particularly important. In recent years, some researchers have used adaptive control and sliding mode control methods for trajectory tracking control research, achieving certain results. However, most of the studies are based on kinematics, with only a few based on dynamics[3]. Most studies use sliding mode control for skid-steering motion control[4]. In this paper, a dynamic model of a skid-steering vehicle is established, and a model predictive control algorithm is used for trajectory tracking control of the vehicle. The effectiveness of this controller is verified through combined simulations using CarSim and Simulink

2. Vehicle dynamics model and controller design

2.1. Dynamic Model of Small Four-Wheel Slip Steering Unmanned Vehicle

When the unmanned vehicle is driving outdoors, the forces it experiences generally include the friction between the wheels and the ground, the driving force of the motor, and the air resistance. The force between various mechanisms inside the vehicle is very complex. Therefore, based on the actual vehicle structure and the objective motion process, the following assumptions are made[5]:

ISSN: 2664-9640

(1) Due to the small impact of the suspension on the vehicle, the influence of the suspension on the vehicle's motion is ignored.

(2) Since the vehicle is mostly in a linear state during normal driving, it is assumed that the tires are in a linear state.

(3) Due to the small air resistance during low-speed operation, this paper ignores air resistance.

(4) Since the center of the vehicle almost coincides with the center of the chassis, the variation of the left and right loads of the chassis is ignored. According to the above assumptions, the dynamic model of the vehicle is shown in Figure 1.

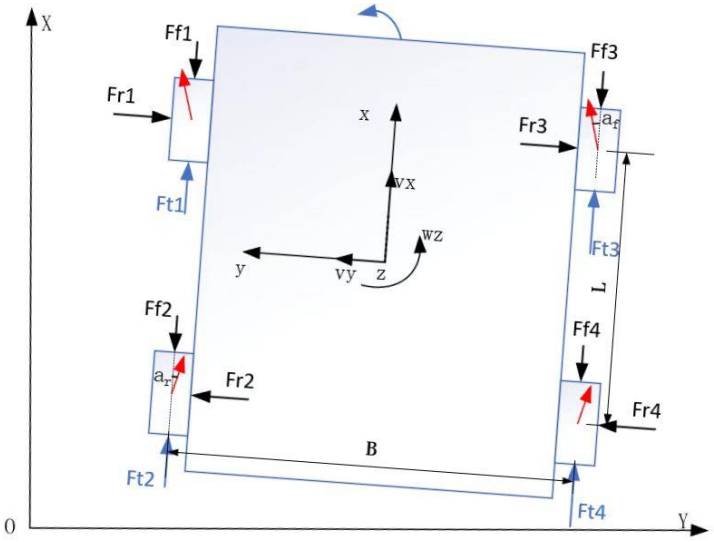

Figure 1 :Slip-Turn Chassis Kinematic Model.

The coordinate systems are converted to facilitate the description of the body state and motion path of unmanned platforms, establishing the vehicle coordinate system oxy and the earth coordinate system OXY. The origin O is set at the initial position of the vehicle's center on the ground, and the origin o is set at the position of the vehicle's center of gravity[6-7]. The angle between X and x is r. In the process of tracking the vehicle's trajectory, it is necessary to observe the relationship between the vehicle's motion path and the desired path, namely the longitudinal, lateral and yawing motion of the vehicle in the plane.

$$\begin{bmatrix} \dot{X} \\ \dot{Y} \\ \dot{\psi} \end{bmatrix} = \begin{bmatrix} \cos\gamma & -\sin\gamma & 0 \\ \sin\gamma & \cos\gamma & 0 \\ 0 & 0 & 1 \end{bmatrix} \begin{bmatrix} \dot{x} \\ \dot{y} \\ \dot{\varphi} \end{bmatrix} \quad (1)$$

Table 1 :Model Parameters

Parameter Name	The meaning of the parameters
z	Center of gravity of the vehicle
B	Wheelbase of the vehicle
L	Axle distance of the vehicle
vx	Longitudinal velocity of the center of gravity
vy	Lateral velocity of the center of gravity
wz	Yaw rate of the vehicle
Fr1, Fr2, Fr3, Fr4	Lateral forces on the four wheels of the vehicle
Ff1, Ff2, Ff3, Ff4	Rolling resistance on the four wheels of the vehicle
Ft1, Ft2, Ft3, Ft4	Driving forces on the four wheels of the vehicle

ISSN: 2664-9640

The force balance equations for the x-axis, y-axis, and z-axis rotation can be obtained from Newton's second law.

When the vehicle is turning, the force equation is:

$$\begin{cases} m\ddot{x} = F_{t1} + F_{t2} + F_{t3} + F_{t4} - mgf \\ m\ddot{y} = F_{r1} + F_{r3} - F_{r2} - F_{r4} \\ I_z\ddot{\theta} = (F_{t4} + F_{t3} - F_{t2} - F_{t1}) * \frac{B}{2} + (F_{f1} + F_{f2} - F_{f3} - F_{f4}) * \frac{B}{2} - \\ (F_{r4} + F_{r2} - F_{r1} - F_{r3}) * \frac{L}{2} \\ \dot{Y} = v_x * \sin\varphi + v_y * \cos\varphi \\ \dot{X} = v_x * \cos\varphi - v_y * \sin\varphi \end{cases} \quad (2)$$

The magic formula tire model:

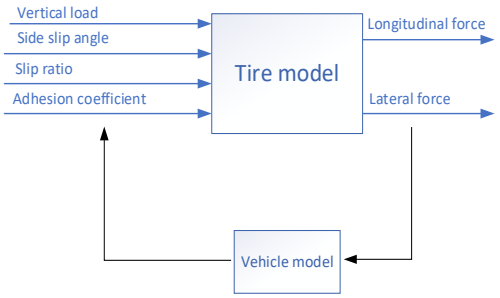

Figure 2 :Tire side slip characteristic model

In the actual motion of the vehicle, the tire is the only component in contact with the ground. Various forces acting on the tire affect the turning characteristics and driving stability of the car. Therefore, it is necessary to establish an accurate tire model that reflects the tire's side slip characteristics to further improve the vehicle dynamics model. The magic formula-based empirical tire model has been widely used in the automotive industry due to its high precision, fast formula solving speed, and other advantages[7-8]. In this paper, the magic formula tire model is selected, and its principle is shown in Figure 2. By inputting relevant parameters of the vehicle during driving and then calculating, the longitudinal force and lateral force of the tire can be obtained.

The magic formula can generally be expressed as:

$$Y(x) = D\sin\{C\arctan[Bx - E(Bx - \arctan(Bx))]\} \quad (3)$$

Where Y is the output, x is the input. When the input variables are the tire's side slip angle or longitudinal slip ratio, the longitudinal force and lateral force can be obtained. The coefficients B, C, D, and E are the magic formula coefficients. When the side slip angle is small, the linear tire model can be used to obtain the longitudinal force and lateral force of the tire:

$$F_{r1} = F_{r3} = C_f * \alpha_f \quad (4)$$

$$F_{r2} = F_{r4} = C_r * \alpha_r \quad (5)$$

Where C_f and C_r are the side slip stiffness of the front and rear tires, respectively.

The side slip angle of the front and rear tires can be expressed as:

$$\alpha_f = \frac{v_y + 0.5Lw_z}{v_x} \quad (6)$$

$$\alpha_r = \frac{v_y - 0.5Lw_z}{v_x} \quad (7)$$

2.2. Trajectory tracking controller design:

The schematic diagram of the MPC trajectory tracking controller is shown in Figure 3. Based on the historical information and future information of the controlled model, it predicts the future output response of the control object. Using a selected parameter metric to achieve

ISSN: 2664-9640

optimization, it solves the optimal control rate for future finite time steps. It also corrects the model-based predicted output based on the actual output of the controlled object and optimizes for the next moment[9-10].

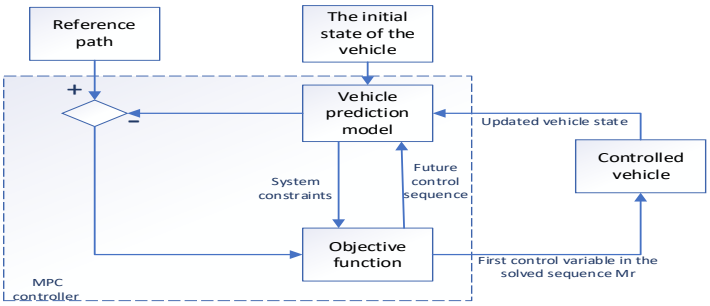

Figure 3: Schematic diagram of MPC trajectory tracking controller

The simplified dynamic model of the unmanned vehicle single track is obtained by simplifying equation (2) as follows:

$$\begin{cases} m\ddot{y} = -m\dot{x}\dot{\varphi} + 2(F_{yf} + F_{yr}) \\ m\ddot{x} = m\dot{y}\dot{\varphi} + F_d \\ I_z\ddot{\varphi} = \frac{L}{2} * 2(F_{yf} - F_{yr}) + M_d \\ \dot{Y} = \dot{x}\sin\varphi + \dot{y}\cos\varphi \\ \dot{X} = \dot{x}\cos\varphi - \dot{y}\sin\varphi \end{cases} \tag{8}$$

In the equation, Fy is the lateral force acting on a single wheel. The lateral speed, longitudinal speed, heading angle, yaw rate, lateral displacement in the global coordinate system, and longitudinal displacement in the global coordinate system are selected as state variables. The desired yaw moment applied to the vehicle body is selected as the control variable. The longitudinal forces of the tires provide the steering drive moment, while the lateral force and rolling friction force provide the steering resistance moment.

Steering resistance moment caused by rolling friction:

$$M_{f1} = Mgf \times \frac{B}{2} \tag{9}$$

Steering drive moment under current adhesion conditions:

$$M_t = Mg\mu_x \times \frac{B}{2} \tag{10}$$

Maximum value of steering moment that can be provided by longitudinal force during slipping steering:

$$M_z = M_t - M_{f1} \tag{11}$$

When the longitudinal speed is constant at v0, equation (8) gives

$$\begin{cases} m\ddot{y} = -m\dot{x}\dot{\varphi} + 2(F_{yf} + F_{yr}) \\ \dot{x} = \frac{v_0}{3.6} \\ I_z\ddot{\varphi} = \frac{L}{2} * 2(F_{yf} - F_{yr}) + M_z \\ \dot{Y} = \dot{x}\sin\varphi + \dot{y}\cos\varphi \\ \dot{X} = \dot{x}\cos\varphi - \dot{y}\sin\varphi \end{cases} \tag{12}$$

the state variables.: $\dot{y}, \dot{x}, \varphi, \dot{\varphi}, Y, X$.

By substituting equations (4)-(7) into equation (12), we have:

ISSN: 2664-9640

$$\begin{cases} m\ddot{y} = -m\dot{x}\dot{\varphi} + 2\left[C_{cf} \times \left(\frac{\dot{y}+0.5\times\dot{\varphi}L}{\dot{x}}\right) - C_{cr} \times \left(\frac{\dot{y}-0.5\times\dot{\varphi}L}{\dot{x}}\right)\right]) \\ \dot{x} = \frac{v_0}{3.6} \\ I_z\ddot{\varphi} = \frac{L}{2} * 2\left(-C_{cf} \times \left(\frac{\dot{y}+0.5\times\dot{\varphi}L}{\dot{x}}\right) - C_{cr} \times \left(\frac{\dot{y}-0.5\times\dot{\varphi}L}{\dot{x}}\right)\right) + M_d \\ \dot{Y} = \dot{x}\sin\varphi + \dot{y}\cos\varphi \\ \dot{X} = \dot{x}\cos\varphi - \dot{y}\sin\varphi \end{cases} \tag{13}$$

Here, we assume that the longitudinal speed v0 is constant. The purpose of trajectory tracking is to make the vehicle's yaw angle and lateral position approach the reference trajectory, so the nonlinear model is obtained as follows:

$$\begin{cases} \dot{\xi} = f(\xi, u) \\ \eta = h(\xi) \end{cases} \tag{14}$$

As mentioned above, in this system, the state variable is chosen as $\dot{\xi} = [\dot{y}, \dot{x}, \varphi, \dot{\varphi}, Y, X]$; the control variable is u=Mz. The output variable is chosen as $\eta = [\varphi, Y]^T$.In the actual control process, the road adhesion coefficient is considered as a known quantity.

2.2.1. Linearization and discretization of the dynamic model

In this study on the motion of a slip-turning vehicle, a linear time-varying model predictive control algorithm is adopted. Since the dynamic model established in this study is a nonlinear system, it needs to be linearized and discretized. The forward Euler method is used to discretize the nonlinear formula at time k;

$$\xi(k+1) = \xi(k) + T * f\big(\xi(k), u(k)\big) \tag{15}$$

The above equation (15) can be simplified as follows:

$$\xi(k+1) = F[\xi(k), u(k)] \tag{16}$$

To linearize equation (16), it is expanded using a Taylor series at a certain operating point:

$$\xi(k+1) = F[\hat{\xi}_0(k), u_0(k)] + \frac{\partial F}{\partial \xi}\Big|_{\xi_0(k),u_0(k)}(\xi(k) - \hat{\xi}_0(k)) + \frac{\partial F}{\partial u}\Big|_{\xi_0(k),u_0(k)}(u(k) - u_0(k)) \tag{17}$$

$$A_{k,0} = \frac{\partial F}{\partial \xi}\Big|_{\xi_0(k),u_0(k)}, \quad B_{k,0} = \frac{\partial F}{\partial u}\Big|_{\xi_0(k),u_0(k)} \tag{18}$$

Then equation (17) becomes:

$$\xi(k+1) = F[\hat{\xi}_0(k), u_0(k)] + A_{k,0}(\xi(k) - \hat{\xi}_0(k)) + B_{k,0}(u(k) - u_0(k)) \tag{19}$$

Equation (16) can be written as:

$$\hat{\xi}(k+1) = F\big[\hat{\xi}(k), u(k)\big] \tag{20}$$

By subtracting equation (19) from equation (20), we obtain:

$$\begin{cases} \xi(k+1) = A_{k,0}\xi(k) + B_{k,0}u(k) + d_{k,0}(k) \\ d_{k,0}(k) = \hat{\xi}(k+1) - A_{k,0}\hat{\xi}_0(k) - B_{k,0}u_0(k) \end{cases} \tag{21}$$

Expanding at any point(ξ_t, u_t), we get:

$$\begin{cases} \xi(k+1) = A_{k,t}\xi(k) + B_{k,t}u(k) + d_{k,t}(k) \\ d_{k,t}(k) = \hat{\xi}(k+1) - A_{k,t}\hat{\xi}_t(k) - B_{k,t}u_t(k) \end{cases} \tag{22}$$

The above equation is the linear time-varying predictive model, but it does not include the control increment, which means it cannot be constrained by the control increment, leading to excessive variation in yaw moments. Therefore, it is processed as follows:

ISSN: 2664-9640

$$\xi_{new}(k+1) = \begin{bmatrix} \xi(k+1) \\ u(k) \end{bmatrix} \tag{23}$$

$$\xi_{new}(k+1) = \begin{bmatrix} A_{k,t}\xi(k) + B_{k,t}\big(u(k-1) + \Delta u(k)\big) + d_{k,t}(k) \\ u(k-1) + \Delta u(k) \end{bmatrix} \tag{24}$$

$$= \begin{bmatrix} A_{k,t} & B_{k,t} \\ 0 & 1 \end{bmatrix} \begin{bmatrix} \xi(k) \\ u(k-1) \end{bmatrix} + \begin{bmatrix} B_{k,t} \\ 1 \end{bmatrix} \Delta u(k) + \begin{bmatrix} d_{k,t} \\ 0 \end{bmatrix}$$

Let: $A = \begin{bmatrix} A_{k,t} & B_{k,t} \\ 0 & 1 \end{bmatrix}$, $B = \begin{bmatrix} B_{k,t} \\ 1 \end{bmatrix}$, $d_k = \begin{bmatrix} d_{k,t} \\ 0 \end{bmatrix}$;

$$\begin{cases} \xi_{new}(k+1) = A\xi_{new}(k) + B\Delta u(k) + d_k \\ \eta(k) = C\xi_{new}(k) = \begin{bmatrix} \varphi(k) \\ Y(k) \end{bmatrix} \end{cases} \tag{25}$$

2.3. The model prediction objective function design

The objective function is set as:

$$J = \sum_{i=1}^{N_p} \left|\left|\eta(t+i|t) - \eta_{ref}(t+i|t)\right|\right|^2 Q + \sum_{i=1}^{N_c} \left|\left|\Delta u(t+i|t)\right|\right|^2 R + \rho\varepsilon^2 \tag{26}$$

Due to the complexity of the vehicle dynamics model and the presence of various constraints, it may not be possible to obtain an optimal solution within a given time during the execution of the controller. To avoid this situation, a relaxation factor ρ is added to the objective function.

According to equation (26), we have:

$$\begin{cases} \xi_{new}(k+2) = A^2\xi_{new}(k) + AB\Delta u(k) + B\Delta u(k+1) + Ad_k + d_{k+1} \\ \xi_{new}(k+3) = A^3\xi_{new}(k) + A^2B\Delta u(k) + AB\Delta u(k+1) + B\Delta u(k+2) + A^2d_k + Ad_{k+1} + d_{k+2} \\ \cdots\cdots \\ \xi_{new}\big(k+N_p\big) = A^{N_p}\xi_{new}(k) + A^{N_p-1}B\Delta u(k) + \cdots + B\Delta u\big(k+N_p-1\big) + A^{N_p-1}d_k + \\ A^{N_p-2}d_{k+1} + \cdots + d_{k+N_p-1} \end{cases} \tag{27}$$

According to $\eta(k) = C\xi_{new}(k)$:

$$Y(t) = \begin{bmatrix} \eta(k+1) \\ \eta(k+2) \\ \cdots \\ \eta\big(k+N_p\big) \end{bmatrix} = C \begin{bmatrix} \xi_{new}(k+1) \\ \xi_{new}(k+2) \\ \cdots \\ \xi_{new}\big(k+N_p\big) \end{bmatrix} \tag{28}$$

Simplifying, we have:

$$Y(t) = \psi_t\xi_{new}(t) + \theta_t\Delta u(t) + \Gamma_t\Phi(t) \tag{29}$$

where:

$$\psi_t = \begin{bmatrix} CA \\ CA^2 \\ \vdots \\ CA^{N_p} \end{bmatrix};\ \theta_t = \begin{bmatrix} CB & & & \\ CAB & CB & & \\ \vdots & \vdots & \ddots & \\ CA^{N_p-1}B & CA^{N_p-2}B & \cdots & CA^{N_p-N_c}B \end{bmatrix}_{N_p \times N_c};$$

$$\Delta u(t) = \begin{bmatrix} \Delta u(k) \\ \Delta u(k+1) \\ \vdots \\ \Delta u(k+N_c-1) \end{bmatrix};\ \Gamma_t = \begin{bmatrix} C & & & \\ CA & CB & & \\ \vdots & \vdots & \ddots & \\ CA^{N_p-1} & CA^{N_p-2} & \cdots & C \end{bmatrix};$$

ISSN: 2664-9640

$$\Phi(t)=\begin{bmatrix} d_k \\ d_{k+1} \\ \vdots \\ d_{k+N_p-1} \end{bmatrix};$$

$$\text{Let } Y(t)=\begin{bmatrix} \eta(t+1) \\ \eta(t+2) \\ \cdots \\ \eta(t+N_p) \end{bmatrix};\ Y_{ref}(t)=\begin{bmatrix} \eta_{ref}(t+1) \\ \eta_{ref}(t+2) \\ \cdots \\ \eta_{ref}(t+N_p) \end{bmatrix};\ \Delta U=\begin{bmatrix} \Delta u(t) \\ \Delta u(t+1) \\ \vdots \\ \Delta u(t+N_c-1) \end{bmatrix};$$

$$J=[Y-Y_{ref}]^T\overline{Q}[Y-Y_{ref}]+\Delta U^T\overline{R}\Delta U+\varepsilon^T\rho\varepsilon \tag{30}$$

$$\text{where } \overline{Q}=\begin{bmatrix} Q & & \\ & \ddots & \\ & & Q \end{bmatrix};\ \overline{R}=\begin{bmatrix} R & & \\ & \ddots & \\ & & R \end{bmatrix};$$

Substituting Equation (29) into Equation (30), we have:

$$J=[\psi_t\xi_{new}(t)+\theta_t\Delta u(t)+\Gamma_t\Phi(t)-Y_{ref}]^T\overline{Q}[\psi_t\xi_{new}(t)+\theta_t\Delta u(t)+\Gamma_t\Phi(t)-Y_{ref}]+\Delta U^T\overline{R}\Delta U+\varepsilon^T\rho\varepsilon \tag{31}$$

Let $E=Y_{ref}-\psi_t\xi_{new}(t)-\Gamma_t\Phi(t)$,

Simplifying the above equation, we obtain:

$$J=\Delta U^T(\theta^T\overline{Q}\theta+\overline{R})\Delta U-2E^T\overline{Q}\theta\Delta U+E^T\overline{Q}E+\varepsilon^T\rho\varepsilon \tag{32}$$

Converting J to the standard form of quadratic programming:

$$\begin{cases} \min\frac{1}{2}X^THX+f^TX \\ s.t.\ AX\le b \end{cases} \tag{33}$$

Since the term $E^T\overline{Q}E$ in the equation has no effect on the optimization of ΔU, we will ignore this term below.

Constructing:

$$X=\begin{bmatrix}\Delta U\\ \varepsilon\end{bmatrix};\ H=\begin{bmatrix}2\theta^T\overline{Q}\theta+2\overline{R} & 0\\ 0 & 2\rho\end{bmatrix};\ f^T=[-2E^T\overline{Q}\theta \quad 0];$$

The standard form of quadratic programming is as follows, where the unknown vector X has been augmented from a one-dimensional vector M to a two-dimensional augmented matrix.

$$J=\frac{1}{2}[\Delta U \quad \varepsilon]H\begin{bmatrix}\Delta U\\ \varepsilon\end{bmatrix}+f^T\begin{bmatrix}\Delta U\\ \varepsilon\end{bmatrix} \tag{34}$$

Constraint design: Constraint design includes three parts, namely constraints on the control variable u(k), constraints on the output variables φ(k), and constraints on Y(k). Constraints on the control variable u(k):

$$\begin{gathered} u(k)=u(k-1)+\Delta u(k) \\ u(k+1)=u(k-1)+\Delta u(k)+\Delta u(k+1) \\ \cdots \\ u(k+N_c-1)=u(k-1)+\Delta u(k)+\Delta u(k+1)+\cdots+\Delta u(k+N_c-1) \end{gathered} \tag{35}$$

ISSN: 2664-9640

$$U = \begin{bmatrix} u(k) \\ u(k+1) \\ \vdots \\ u(k+N_c-1) \end{bmatrix} = \begin{bmatrix} u(k-1) \\ u(k-1) \\ \vdots \\ u(k-1) \end{bmatrix} + \begin{bmatrix} I & & & \\ I & I & & \\ \vdots & \vdots & \ddots & \\ I & I & \cdots & I \end{bmatrix} \begin{bmatrix} \Delta u(k) \\ \Delta u(k+1) \\ \vdots \\ \Delta u(k+N_c-1) \end{bmatrix} \tag{36}$$

Let : $U_t = \begin{bmatrix} u(k-1) \\ u(k-1) \\ \vdots \\ u(k-1) \end{bmatrix}$; $A_I = \begin{bmatrix} I & & & \\ I & I & & \\ \vdots & \vdots & \ddots & \\ I & I & \cdots & I \end{bmatrix}$; $\Delta U = \begin{bmatrix} \Delta u(k) \\ \Delta u(k+1) \\ \vdots \\ \Delta u(k+N_c-1) \end{bmatrix}$

be rearranged :

$$U = U_t + A_I \Delta U \tag{37}$$

$$\begin{bmatrix} u_{min} \\ u_{min} \\ \vdots \\ u_{min} \end{bmatrix} \le \begin{bmatrix} u(k) \\ u(k+1) \\ \vdots \\ u(k+N_c-1) \end{bmatrix} \le \begin{bmatrix} u_{max} \\ u_{max} \\ \vdots \\ u_{max} \end{bmatrix} \tag{38}$$

From the above equation, we can obtain:

$$U_{min} \le U_t + A_I \Delta U \le U_{max} \tag{39}$$

Simplifying the above equation, we have:

$$\begin{cases} A_I \Delta U \le U_{max} - U_t \\ -A_I \Delta U \le -U_{min} + U_t \end{cases} \tag{40}$$

Constraints on the control increment Δu:

$$\begin{cases} \Delta u_{min} \le \Delta u \le \Delta u_{max} \\ 0 \le \varepsilon \le M \end{cases} \tag{41}$$

Simplifying, we have:

$$\begin{bmatrix} \Delta u_{min} \\ 0 \end{bmatrix} \le \begin{bmatrix} \Delta u \\ \varepsilon \end{bmatrix} \le \begin{bmatrix} \Delta u_{max} \\ M \end{bmatrix} \tag{42}$$

Let $l_b = \begin{bmatrix} \Delta u_{min} \\ 0 \end{bmatrix}$; $u_b = \begin{bmatrix} \Delta u_{max} \\ M \end{bmatrix}$;

be rearranged :

$$l_b \le \Delta U \le u_b \tag{43}$$

Constraints on the output variables φ(k) and Y(k):

$$Y_{min} \le Y \le Y_{max}$$

$$Y_{min} \le \psi_t \xi_{new}(t) + \theta_t \Delta u(t) + \Gamma_t \Phi(t) \le Y_{max}$$

$$\begin{cases} \theta_t \Delta u(t) \le Y_{max} - \psi_t \xi_{new}(t) - \Gamma_t \Phi(t) \\ -\theta_t \Delta u(t) \le -Y_{min} + \psi_t \xi_{new}(t) + \Gamma_t \Phi(t) \end{cases}$$

Simplifying, we have:

$$\begin{bmatrix} \theta & 0 \\ -\theta & 0 \end{bmatrix} \begin{bmatrix} \Delta U \\ \varepsilon \end{bmatrix} \le \begin{bmatrix} Y_{max} - \psi_t \xi_{new}(t) - \Gamma_t \Phi(t) \\ -Y_{min} + \psi_t \xi_{new}(t) + \Gamma_t \Phi(t) \end{bmatrix} \tag{44}$$

Combining the above constraints, we have:

$$\begin{bmatrix} A_I & 0 \\ -A_I & 0 \\ \theta & 0 \\ -\theta & 0 \end{bmatrix} \begin{bmatrix} \Delta U \\ \varepsilon \end{bmatrix} \le \begin{bmatrix} U_{max} - U_t \\ -U_{min} + U_t \\ Y_{max} - \psi_t \xi_{new}(t) - \Gamma_t \Phi(t) \\ -Y_{min} + \psi_t \xi_{new}(t) + \Gamma_t \Phi(t) \end{bmatrix} \tag{45}$$

Let : $A_{cons} = \begin{bmatrix} A_I & 0 \\ -A_I & 0 \\ \theta & 0 \\ -\theta & 0 \end{bmatrix}$; $B_{cons} = \begin{bmatrix} U_{max} - U_t \\ -U_{min} + U_t \\ Y_{max} - \psi_t \xi_{new}(t) - \Gamma_t \Phi(t) \\ -Y_{min} + \psi_t \xi_{new}(t) + \Gamma_t \Phi(t) \end{bmatrix}$

ISSN: 2664-9640

be rearranged :

$$A_{cons} \cdot \Delta U \leq B_{cons} \tag{46}$$

$$\begin{cases} l_b \leq \Delta U \leq u_b \\ A_{cons} \cdot \Delta U \leq B_{cons} \end{cases} \tag{47}$$

3. Simulation analysis and result comparison

3.1. Joint simulation of Carsim and Matlab/Simulink

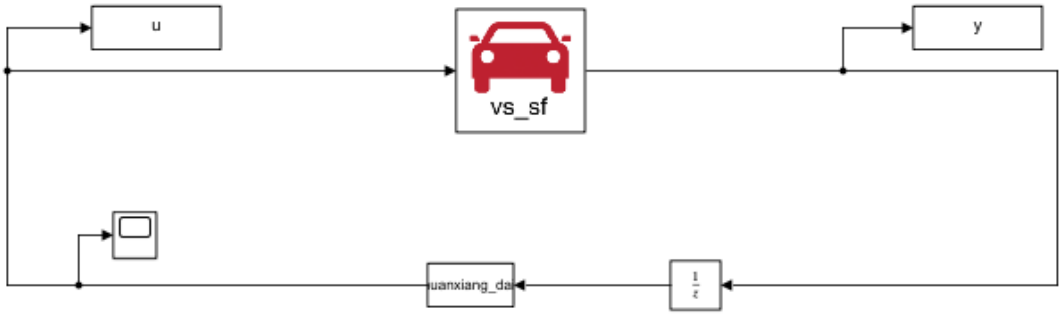

Figure 4: Joint Simulation Diagram

Simulation result analysis:

In order to verify the effectiveness of the MPC trajectory tracking control method, a joint simulation experiment was conducted using Carsim and Matlab/Simulink software. The relevant parameters of the vehicle model were set in Carsim for road simulation, and the trajectory tracking controller was designed in Matlab/Simulink. This method has relatively high fidelity in simulating the effects. The main simulation parameters of the vehicle are as follows: total vehicle mass is 144 kg; distance from the center of mass to the front and rear axles is 0.4m; the moment of inertia of the vehicle rotating around the center of mass, Iz, is 25 (kg·m^2); the distance between the front and rear wheels is 0.75m; and the height of the center of mass is 0.35m.

The simulated vehicle travels at a constant speed of 15km/h on a road surface with good adhesion conditions (friction coefficient of 0.85), and the effect of the vehicle tracking the double trajectory is shown in the figure.

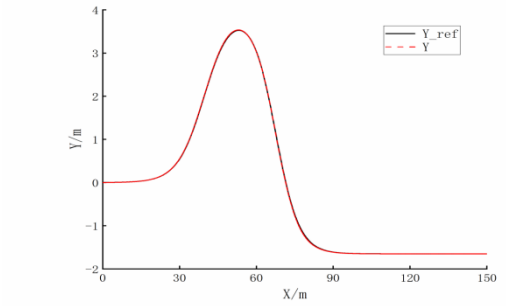

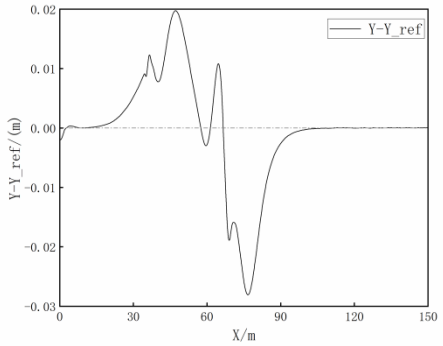

Figure 5: Trajectory Tracking Curve Figure 6: Trajectory Tracking Error Curve

From Figure 5, it can be seen that the designed trajectory tracking controller has good tracking effect on the lateral position of the double trajectory. From Figure 6, it can be seen that the maximum error of lateral tracking during trajectory tracking by the controller does not exceed 0.03m. The vehicle's trajectory tracking error is within an allowable range, indicating good stability.

ISSN: 2664-9640

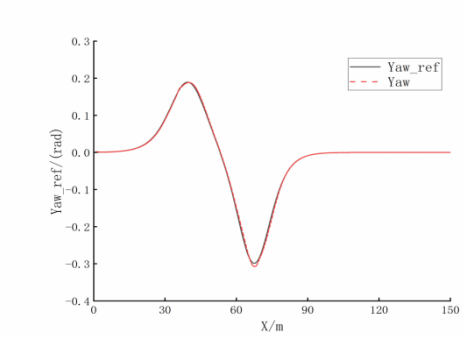

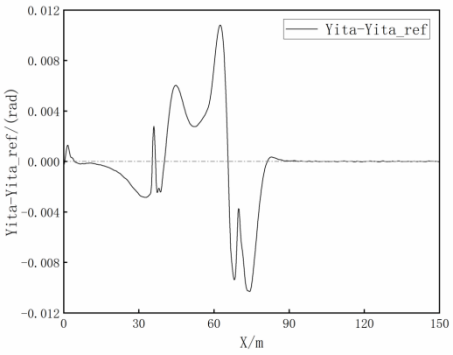

Figure 7: Yaw Angle Tracking Curve Figure 8: Yaw Angle Tracking Error Curve

The trajectory tracking controller designed in Figure 7 has good tracking performance for the lateral yaw angle of double-track. Figure 8 shows that the maximum tracking error in lateral direction during trajectory tracking with this controller does not exceed 0.012 rad. The steering control capability of the vehicle is excellent and can achieve the desired steering angle.

In conclusion, the MPC-based four-wheel slip steering dynamic trajectory tracking controller discussed in this paper can achieve good accuracy and stability during the control process.

4. Conclusion

In conclusion, this paper proposes an MPC-based wheel slip steering vehicle trajectory tracking control method. By establishing the vehicle dynamics model and combining with dynamic constraints, a wheel slip steering trajectory tracking controller based on model predictive control is designed to achieve trajectory tracking and stable driving of the vehicle. The proposed method is validated through joint simulation experiments using Carsim and Matlab/Simulink, and the simulation results show that the proposed method can achieve stable driving and excellent trajectory tracking performance. This method can provide new ideas and references for the control study of wheel slip steering vehicles.

References

[1] X.Y. Wang: Research on Slip Steering and Driving Coordination Control of Distributed Drive Unmanned Platform (MS., Jilin University, China 2021), p.46.

[2] H.W. JIANG: Research on Trajectory Tracking Control for Intelligent Vehicles (MS., Jilin University, China 2019), p.28

[3] J.W. Gong, Y Jiang,W Xu: Model Predictive Control of Autonomous Vehicle (Beijing Institute of Technology Press, China 2014).

[4] A.D. Li: Research on Key Technologies of Autonomous Motion of Mobile Robots in Outdoor Environments (MS., Hebei University of Technology, China 2016), p.35.

[5] S. Wang: Research on Slip Steering Control Strategy of Independent Drive Unmanned Platform (MS.,Jilin University, China 2019),p.50.

[6] M. ELBANHAWI, M. SIMIC, R. JAZAR: Receding horizon lateral vehicle control for pure pursuit path tracking, Journal of Vibration and Control, Vol. 24 (2018) No.3, p.619-642.

[7] J.X. JIANG, P.L. SHI, L.H. ZHOU, L. ZHANG. Path Tracking Control of Intelligent Vehicle with Variable Preview Distance, Journal of Shandong University of Technology (Natural Science Edition), Vol. 35 (2021) No.4, p.70-74+80.

[8] M. CHOI, S.B. CHOI: MPC for vehicle lateral stability via differential braking and active front steering considering practical aspects, Proceedings of the Institution of Mechanical Engineers, Part D: Journal of Automobile Engineering, Vol. 230 (2016) No.4, p.4599-469.2

ISSN: 2664-9640

[9] S. XU, H. PENG: Design, analysis, and experiments of preview path tracking control for autonomous vehicles, IEEE Transactions on Intelligent Transportation Systems, Vol. 21 (2019) No.1, p.48-58.

[10] L. CHEN, Z.B. QIN, W.W KONG, X. CHEN. LQR Lateral Control of Intelligent Vehicle Based on Optimal Front Wheel Side Deflection Force, Journal of Tsinghua University (Natural Science), Vol.61 (2021) No.9, p.906-912.